PHYSICAL REVIEW B **94**, 241115(R) (2016)

Critical metal-insulator transition due to nuclear quantum effects in Mn-doped GaAs

Soungmin Bae and Hannes Raebiger*
Department of Physics, Yokohama National University, Yokohama, Japan
(Received 13 September 2016; revised manuscript received 15 November 2016; published 27 December 2016)

Mn-doped GaAs exhibits a critical metal-insulator transition at the Mn concentration of $x_{\mathrm{crit}} \approx 1\%$. Our self-interaction corrected first principles calculation shows that for Mn concentrations $x \gtrsim 1\%$, hole carriers are delocalized in host valence states, and for $x \lesssim 1\%$, holes tend to be trapped in impurity-band-like states. We further show that for a finite range of concentrations around x_{crit} the system exhibits a nonadiabatic superposition of these states, i.e., a mixing of electronic and nuclear wave functions. This means that the phase transition is continuous, and its criticality is caused by quantum effects of the atomic nuclei. In other words, the apparently *electronic* phase transition from the insulator to metal state cannot be described by electronic effects alone.

DOI: 10.1103/PhysRevB.94.241115

Fundamental theories for metal-insulator transitions were laid out half a century ago [1–4], but the electronic structures and correlations underlying such transitions remain unknown. $Ga_{1-x}Mn_xAs$ exhibits a critical metal-insulator transition at around $x_{\mathrm{crit}} \approx 1\%$ [5], accompanied with the emergence of carrier-mediated ferromagnetism for metallic samples with Mn concentrations $x > 1\%$ [6–8]. The carrier holes, however, exhibit the duality of both being trapped in impurity band states [9–13] and being delocalized in conductive valence band states [7,8,14–17], leaving the ground state of $Ga_{1-x}Mn_xAs$ unresolved [18]. Our first principles calculation of $Ga_{1-x}Mn_xAs$ describes both types of hole states, and shows that for a range of concentrations around x_{crit} the system exhibits a nonadiabatic superposition of these states. This means that electronic wave functions get correlated with nuclear wave functions. Once the atomic nuclei are given a full quantum mechanical treatment, we can generalize the theory of excitonic insulators [3,19–21] (formally similar to the BCS theory of superconductivity [22]) to describe the critical metal-insulator transition of $Ga_{1-x}Mn_xAs$. Now, neither the ground state nor phase transition can be described without nuclear wave functions, and the paradigm that electronic properties of a metal or insulator can be described by its electrons falls apart.

First principles calculations of $Ga_{1-x}Mn_xAs$ support either impurity band [23] or valence band [14,15] models, but are prone to systematic failures [24] and have not been able to reproduce experimentally observed wave functions [5,25,26]. In order to avoid these pitfalls, we apply a self-interaction correction (SIC) [27] to our density-functional calculation of $Ga_{1-x}Mn_xAs$ nearby the metal-insulator transition. This SIC is implemented by a hole-state potential ($\lambda = 4.4$ eV) acting on As p electrons, chosen to satisfy the generalized Koopmans' condition [27]. We carry out our calculations using the projector augmented-wave method implemented in the VASP code [28] with the generalized gradient approximation Perdew-Burke-Ernzerhof functional, including an on-site correction for Mn d levels ($U = 3.9$ eV and $J = 1.0$ eV) [29]. Plane waves are included up to the cutoff energy of 275 eV, and atomic structures are relaxed until the forces on each atom are below 0.005 eV/Å. Our $Ga_{1-x}Mn_xAs$ systems are described in cubic and fcc shaped supercells of 216 and 432 atoms with $2\times2\times2$ and Γ-only Brillouin zone samplings, respectively. One Ga atom in the center of the cell is replaced by Mn, yielding Mn concentrations of $x = 0.93\%$ and $x = 0.46\%$.

Our calculated hole states (shown in Fig. 1) exhibit a *bowtielike* feature, as observed experimentally [5,25,26] (Fig. 2). Previous attempts to describe $Ga_{1-x}Mn_xAs$ from first principles yield symmetric hole distributions (see, e.g., Refs. [23,30]) with a triangular envelope function, and fail to reproduce this bowtielike feature due to spurious self-interaction errors in local-density functionals [24]. Previous SIC calculations [31–34] have only studied very small systems ($\leqslant$64 atoms), which is not sufficient for comparison with scanning tunneling microscopy (STM) images. In addition to reproducing the STM topographies, our very dilute systems with $x = 0.93\%$ and $x = 0.46\%$ show two stationary states, both of which exhibit similar bowtielike features in the (110) plane, but differ in contrast [bright features labeled I shown in Figs. 1(a)–1(d); less bright M in Figs. 1(e)–1(h)]. A similar variation in brightness can be seen in the STM topographic images of Richardella *et al.* [5] shown in Fig. 2; notice that the relative abundance of the different brightness features seems to vary with Mn concentration x.

Figure 3 shows the density of states (DOS) for the two different adiabatic stationary state configurations I [Figs. 3(a) and 3(b)] and M [Figs. 3(c) and 3(d)] for $x = 0.93\%$ (the DOS for $x = 0.46\%$ show the same features). For either state, the main Mn d contribution is about 4 eV below the GaAs valence band edge (set as zero), well in agreement with photoemission experiment [35]. The crucial difference of I and M is shown in Figs. 3(b) and 3(d): The hole state corresponding to the bright bowtie feature of I [Figs. 1(a)–1(d) and 3(a) and 3(b)] is separated by a gap from the valence continuum of states, whereas the hole state corresponding to the less bright feature of M [Figs. 1(e)–1(h) and 3(c) and 3(d)] is merged with the valence band. Thus, I is an insulating state and M a metallic state; the M state agrees well with the previous SIC calculation [31–34], but the I state has not been theoretically described before. The ionization (acceptor) energy of the I state is 0.11 eV, which is in excellent agreement with experimental observations [36]. For both metallic and insulating states, the hole states (lowest unoccupied states) contain a small admixture of Mn d orbitals, but the main contribution is due to As p orbitals, as shown by the projected DOS, given in Figs. 3(b) and 3(d). It is clear that

*hannes@ynu.ac.jp

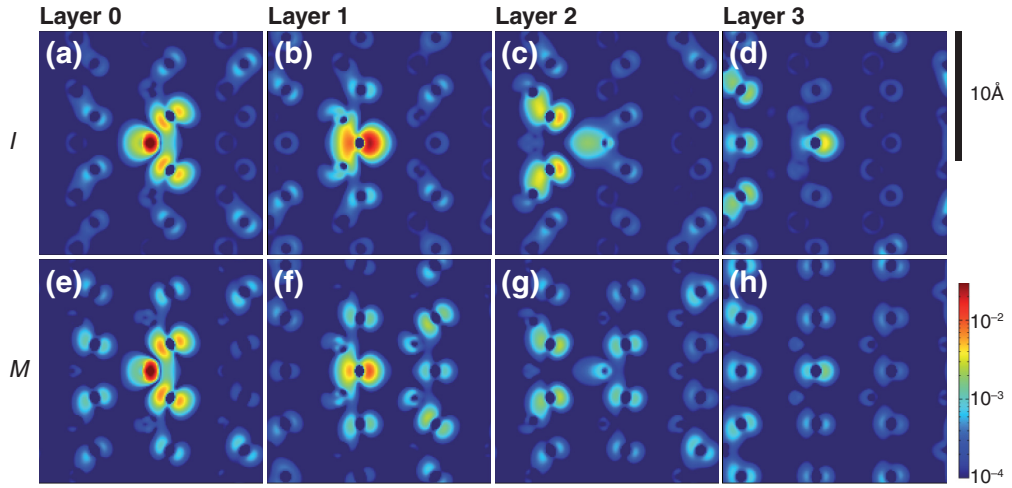

FIG. 1. Local density of states (LDOS) of the unoccupied hole state in the (110) plane calculated for Mn concentration $x = 0.93\%$. (a)–(d) show the more bright feature I; (e)–(h) the less bright feature M. (a) and (e) give the LDOS in the plane containing the Mn impurity (layer 0), (b) and (f) in the layer above it (layer 1), and so on. Scale bars for size and LDOS (units $e/\text{Å}^3$) are given next to the panels.

both types of hole states are best described as host-derived dangling-bond hybrid states [30], i.e., a $d^5 + h$ configuration, but their localization is markedly different. The hole state of the metallic configuration M has a similar amplitude over the four As neighbors of the Mn impurity, while the hole state of the insulator configuration I is pronouncedly localized on one of the neighboring As atoms.

At first glance, neither of the nuclear configurations Q_I nor Q_M, corresponding to the insulating state I and the metallic state M, maintains the host T_d symmetry. The central unit of Mn and its four neighboring As atoms have the C_s and C_{3v} symmetries for the M and I states, respectively. Q_M has two elongated Mn-As bonds and Q_I one elongated Mn-As bond [shown in the insets of Figs. 3(b) and 3(d)]. However, the

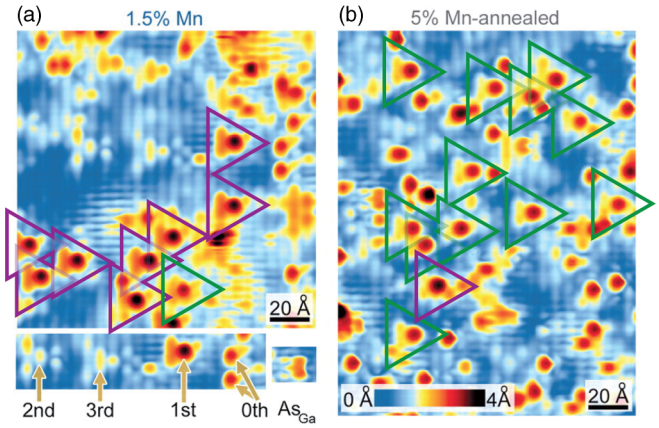

FIG. 2. STM topography of in-gap states of $Ga_{1-x}Mn_xAs$ with (a) $x = 1.5\%$ and (b) $x = 5\%$. The purple and green triangles highlight the first layer subsurface Mn impurities with brighter and less bright contrasts, associated with I and M states, respectively. From Ref. [5]; highlights added by permission. Reprinted with permission from AAAS.

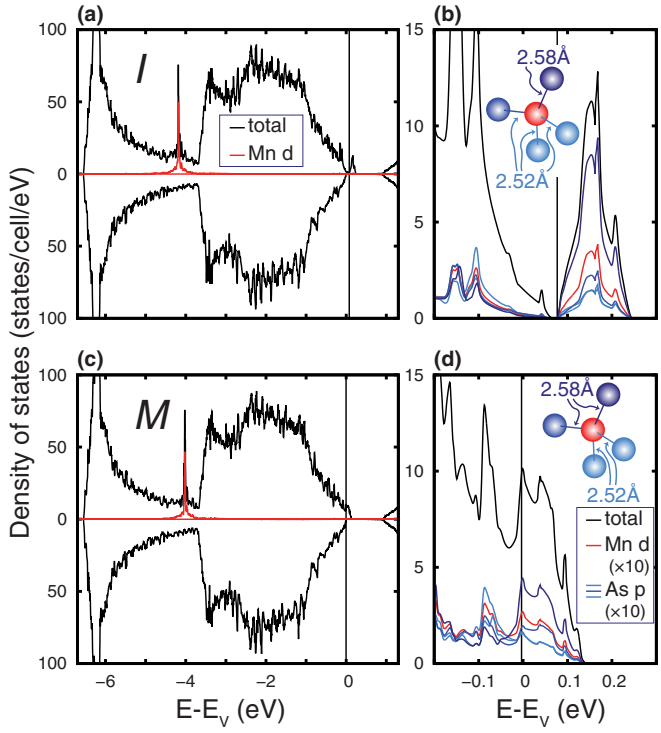

FIG. 3. Density of states (DOS) calculated for Mn concentration $x = 0.93\%$ for (a), (b) insulating state I and (c), (d) metallic state M. (a) and (c) show the majority and minority spin components (majority above 0 and minority below). (b) and (d) show a magnification of the majority spin around the valence band edge $E = E_V$ (set as zero for the horizontal axis). The black line shows the total DOS and the red line the projected density of states (PDOS) on Mn d orbitals. (b) and (d) also give the PDOS of As p orbitals of the As atoms neighboring Mn; the PDOS in (b) and (d) are magnified by 10. The insets of (b) and (d) show the Mn-As interatomic distances, and the different shades of blue used for As p PDOS correspond to the different As atoms indicated by the same color shade in these insets.

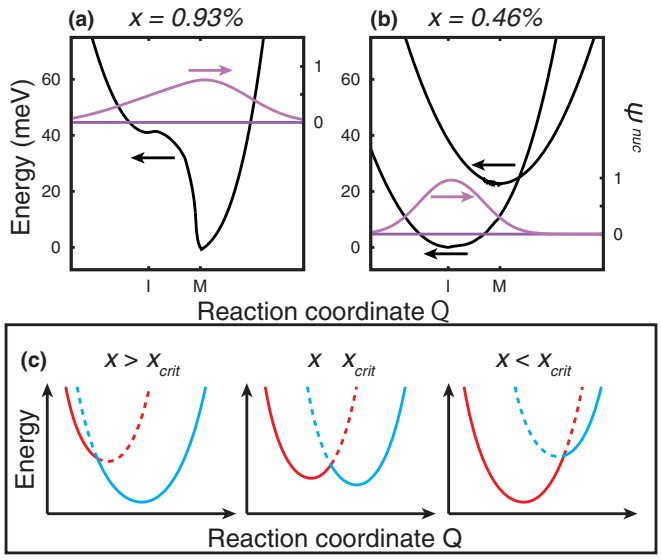

FIG. 4. Adiabatic potential energy curve between metallic (M) and insulator (I) states for (a) $x = 0.93\%$ and (b) $x = 0.46\%$. The horizontal purple lines in (a) and (b) indicate the zero-phonon energy, and the curve above it is the corresponding wave function of nuclear motion $\Psi^{\rm nuc}$. The cartoon in (c) illustrates how the relative stability of metallic (blue) and insulator (red) states evolve as a function of Mn concentration x around the critical value $x_{\rm crit}$.

C_s state of M has six realizations $\{\phi_i^{C_s}\}_{i=1}^6$, which all have the same energy, and we test their stability against structural distortion. We distort the C_s structures towards T_d, and find a very flat adiabatic potential energy curve with a barrier of only $\sim$1 meV, so the metallic state wave function must be described (nonadiabatically) as $\phi^M = \sum_{i=1}^6 \phi_i^{C_s}/\sqrt{6}$, which effectively has the T_d nuclear geometry. The insulating I state, as we show below, exhibits a more complex adiabatic potential landscape, but *can be stable* against such structural distortions. Our finding of two distinctly different $d^5 + h$ configurations, one of which is structurally distorted in the $\langle 111\rangle$ direction, is well in agreement with the electron spin resonance (ESR) observation of two different $d^5 + h$ configurations, one of which is structurally distorted, reported by Masterov *et al.* [37].

Having found two stable minima, the next question is, which one of them is the ground state. For $x = 0.93\%$, the metallic state is lower in energy by 41 meV, whereas for $x = 0.46\%$, the insulator state is lower by 23 meV. This indicates that around $0.5\% < x < 1\%$ the system exhibits a metal-insulator transition, as has been observed experimentally [5,6,11–13,38]. This finding is further corroborated by calculation of 128 and 64 atom supercells, corresponding to $x = 1.6\%$ and $x = 3.1\%$, which only exhibit the metallic state. To elucidate the nature of this metal-insulator transition, we calculate the adiabatic potential energy between metallic and insulator states for $x = 0.93\%$ and $x = 0.46\%$, shown in Fig. 4. The reaction coordinate Q describes the positions of all nuclei in the system, I and M corresponding to geometries for the insulator and metallic states; all other points are obtained by linear interpolation between these configurations, and the potential energy values $V(Q)$ are obtained by fixed geometry calculations at the respective data points. For $x = 0.93\%$ [Fig. 4(a)], M is the ground state, but I and M lie on the same double well $V(Q)$, where at intermediate Q the energy branches corresponding to I to M merge and the electronic structure smoothly transforms from I to M, with a small energy barrier separating the configurations. For $x = 0.46\%$ [Fig. 4(b)], however, I is the ground state, and both configurations have their own adiabatic energy branches V^I and V^M; $V^I < V^M$ also at Q corresponding to M, indicating that M is metastable and may spontaneously decay into I. This finding clarifies why the relative abundance of M states compared with I increases as Mn concentration increases, as can be seen in Fig. 2.

The merging of the adiabatic energy branches and the tiny energy barrier for $x = 0.93\%$ [Fig. 4(a)] suggests that the system should be described by the superposition wave function $\Phi = c_M\phi^M + c_I\phi^I$, where ϕ^M and ϕ^I are wave functions of the metallic and insulator states, respectively. We numerically solve the Schrödingier equation $[-\frac{1}{2m}\frac{\partial^2}{\partial Q^2} + V(Q)]\Psi_i^{\rm nuc} = E_i\Psi_i^{\rm nuc}$ for nuclear motion along the adiabatic potential energies $V(Q)$ [39], obtaining the zero-point energies E_0 and nuclear wave functions $\Psi_0^{\rm nuc}$, shown in Figs. 4(a) and 4(b). Indeed, for $x = 0.93\%$, the zero-point nuclear vibration energy exceeds the potential barrier, and thus the system must be described by the nonadiabatic superposition of metallic and insulator states $\Phi = c_M(Q)\phi^M + c_I(Q)\phi^I$, where the coefficients are functions of the nuclear coordinates Q. The evolution of the adiabatic potential energy landscape is illustrated in the cartoon shown in Fig. 4(c), showing that the expansion coefficients depend also on the Mn concentration x, i.e., $c_I = c_I(Q;x)$ and $c_M = c_M(Q;x)$. For large x, c_I vanishes, and for small x, c_M vanishes, but for a finite range of x, both $c_I(Q)$ and $c_M(Q)$ are nonzero, and the system fluctuates between the metallic and insulator states.

The metal-insulator transition occurs continuously via the superposition state $\Phi = c_M(Q)\phi^M + c_I(Q)\phi^I$ over the finite range of Mn concentrations $x_{\rm crit} - \delta < x < x_{\rm crit} + \delta'$, where both $c_I(Q;x) > 0$ and $c_M(Q,x) > 0$. This type of critical Mott transition was first described by Kohn: [3] For these x, the system exhibits a series of *excitonic phases* [3,4,19–21,40] and has a dielectric ground state formally similar to the BCS ground state [22]. For the insulating state I, exciting an electron to the gap level (forming an electron-hole pair, or exciton) has a finite, nonzero activation energy E_a. However, as x approaches $x_{\rm crit}$ and c_M becomes finite, an excitonic phase with a lower activation energy $\tilde{E}_a < E_a$ emerges, viz., a charge density wave where the charge density fluctuates between conductive and insulator states. At $x_{\rm crit}$ we have an infinity of such excitonic phases, and the activation energy is replaced by the pseudogap $\Delta = 0$ [40], as observed experimentally [5,11–13]. Early work on excitonic phases questioned the very existence of such phases, [20] because changes in the conductive phase (metal versus insulator) must be accompanied by lattice deformations, which may preclude the existence of their superposition state in the adiabatic approximation. Our discovery of the nonadiabatic superposition state $\Phi = c_M(Q)\phi^M + c_I(Q)\phi^I$ in a real physical system thus confirms that excitonic phases and excitonic insulators *do exist*.

For a periodic array of Mn impurities (such as in the present calculation) the excitonic phases exhibit long range order ($|\vec{r} - \vec{r}'| \to \infty$) [21], which explains the divergence in the electron-electron correlation length at the pseudogap energy

seen experimentally [5]. Of course the Mn impurities in realistic experimental samples do not form a periodic array. Both disorder of the impurity distribution and the presence of compensating defects are expected to break some of the charge density waves, which become replaced by random fluctuations [40,41]. However, as discussed by Mott, disorder does not essentially change the nature of the metal-insulator transition: It is continuous due to correlation effects (superposition state $\Phi = c_M\phi^M + c_I\phi^I$) rather than disorder effects, and, near $x_{\rm crit}$ some strong charge density fluctuations with well-defined wave-number and long range order may remain even in disordered systems [40]. In fact, randomness in Mn substitution implies a fluctuation in the local Mn concentration $x_{\rm loc}$, and can be included in the present description by determining the wave-function coefficients c_M and c_I based on $x_{\rm loc}$ rather than the global Mn concentration [$c_I = c_I(Q;x_{\rm loc})$ and $c_M = c_M(Q;x_{\rm loc})$, cf. disorder modified correlations [8,42]]. This implies that for global Mn concentrations much larger or smaller than $x_{\rm crit}$, local pockets can still have $x_{\rm loc} \approx x_{\rm crit}$, which must be described by the nonadiabatic wave function $\Phi(Q,r) = c_M(Q;x_{\rm loc})\phi^M + c_I(Q;x_{\rm loc})\phi^I$. This is consistent with the observations of (i) the coexistence I and M states for a wide range of x (Fig. 2) and (ii) enhanced electron-electron correlation length at the pseudogap energy even for Mn concentrations as large as $x = 5\%$ [5].

We have shown by first principles calculation that $Ga_{1-x}Mn_xAs$ for small x is described by an insulator state with holes trapped in localized impurity band states, and for large x it is in a metallic state with holes delocalized in host valence states. At the critical concentration $0.46\% < x_{\rm crit} < 0.93\%$, $Ga_{1-x}Mn_xAs$ must be described by the nonadiabatic wave function $\Phi(Q,r) = c_M(Q;x_{\rm loc})\phi^M + c_I(Q;_{\rm loc})\phi^I$, where the coefficients c_M and c_I manifest nuclear quantum effects, and ϕ^M and ϕ^I are electronic (adiabatic) wave functions. For the finite range of Mn concentrations $x_{\rm crit} - \delta < x < x_{\rm crit} + \delta'$ where both c_M and c_I are nonzero, the system fluctuates between the metallic and insulator states. Because these fluctuations are due to nuclear quantum effects, $x_{\rm crit}$ and the range parameters δ and δ' should exhibit an isotope effect, similar to BCS superconductors. Moreover, the formal similarity between *excitonic insulator* and BCS theories suggests that similar first principles calculations can also be used for accurate descriptions of superconductors.

We thank A. Ayuela, T. Dietl, K. Ohno, S. Ono, O. Schirmer, K. Shudo, A. Yazdani, D. Yoshida, and A. Zunger for many helpful and inspiring discussions. We thank M. Tachikawa for help with the numerical calculation of vibration modes and nuclear wave functions for anharmonic potentials. S.B. is grateful to the Rotary Yoneyama Memorial Foundation.

[1] N. F. Mott, Proc. Phys. Soc. **62**, 416 (1949).
[2] P. W. Anderson, Phys. Rev. **109**, 1492 (1958).
[3] W. Kohn, Phys. Rev. Lett. **19**, 789 (1967).
[4] N. F. Mott, Rev. Mod. Phys. **40**, 677 (1968).
[5] A. Richardella, P. Roushan, S. Mack, B. Zhou, D. A. Huse, D. D. Awschalom, and A. Yazdani, Science **327**, 665 (2010).
[6] H. Ohno, A. Shen, F. Matsukura, A. Oiwa, A. Endo, S. Katsumoto, and Y. Iye, Appl. Phys. Lett. **69**, 363 (1996).
[7] T. Dietl, H. Ohno, F. Matsukura, J. Cibert, and D. Ferrand, Science **287**, 1019 (2000).
[8] T. Dietl and H. Ohno, Rev. Mod. Phys. **86**, 187 (2014).
[9] S. Ohya, K. Takata, and M. Tanaka, Nat. Phys. **7**, 342 (2011).
[10] M. Dobrowolska, K. Tivakornsasithorn, X. Liu, J. K. Furdyna, M. Berciu, K. M. Yu, and W. Walukiewicz, Nat. Mater. **11**, 444 (2012).
[11] I. Muneta, H. Terada, S. Ohya, and M. Tanaka, Appl. Phys. Lett. **103**, 032411 (2013).
[12] T. Ishii, T. Kawazoe, Y. Hashimoto, H. Terada, I. Muneta, M. Ohtsu, M. Tanaka, and S. Ohya, Phys. Rev. B **93**, 241303 (2016).
[13] I. Muneta, S. Ohya, H. Terada, and M. Tanaka, Nat. Commun. **7**, 1 (2016).
[14] J. Mašek, F. Máca, J. Kudrnovský, O. Makarovsky, L. Eaves, R. P. Campion, K. W. Edmonds, A. W. Rushforth, C. T. Foxon, B. L. Gallagher, V. Novák, J. Sinova, and T. Jungwirth, Phys. Rev. Lett. **105**, 227202 (2010).
[15] I. Di Marco, P. Thunström, M. I. Katsnelson, J. Sadowski, K. Karlsson, S. Lebègue, J. Kanski, and O. Eriksson, Nat. Commun. **4**, 2645 (2013).
[16] S. Prucnal, K. Gao, I. Skorupa, L. Rebohle, L. Vines, H. Schmidt, M. Khalid, Y. Wang, E. Weschke, W. Skorupa, J. Grenzer, R. Hübner, M. Helm, and S. Zhou, Phys. Rev. B **92**, 224407 (2015).
[17] S. Souma, L. Chen, R. Oszwałdowski, T. Sato, F. Matsukura, T. Dietl, H. Ohno, and T. Takahashi, Sci. Rep. **6**, 27266 (2016).
[18] D. G. Andrianov, Y. A. Grigor'ev, S. O. Klimonskĭ, A. S. Saval'ev, and S. M. Yakubenya, Fiz. Tekh. Poluprovodn. **18**, 262 (1984) [Sov. Phys. Semicond. **18**, 162 (1984)].
[19] L. V. Keldysh and Y. V. Kopaev, Fiz. Tverd. Tela **6**, 2791 (1964) [Sov. Phys. Solid State **6**, 2219 (1965)].
[20] W. Kohn, Phys. Rev. Lett. **19**, 439 (1967).
[21] D. Jérome, T. M. Rice, and W. Kohn, Phys. Rev. **158**, 462 (1967).
[22] J. Bardeen, L. N. Cooper, and J. R. Schrieffer, Phys. Rev. **108**, 1175 (1957).
[23] P. Mahadevan, A. Zunger, and D. D. Sarma, Phys. Rev. Lett. **93**, 177201 (2004).
[24] A. Zunger, S. Lany, and H. Raebiger, Physics **3**, 53 (2010).
[25] A. M. Yakunin, A. Y. Silov, P. M. Koenraad, J. H. Wolter, W. Van Roy, J. De Boeck, J.-M. Tang, and M. E. Flatte, Phys. Rev. Lett. **92**, 216806 (2004).
[26] J. K. Garleff, C. Çelebi, W. Van Roy, J.-M. Tang, M. E. Flatté, and P. M. Koenraad, Phys. Rev. B **78**, 075313 (2008).
[27] S. Lany and A. Zunger, Phys. Rev. B **80**, 085202 (2009).
[28] G. Kresse and D. Joubert, Phys. Rev. B **59**, 1758 (1999).
[29] H. Raebiger, S. Lany, and A. Zunger, Phys. Rev. B **79**, 165202 (2009).
[30] H. Raebiger, S. Lany, and A. Zunger, Nature (London) **453**, 763 (2008).
[31] A. Filippetti, N. A. Spaldin, and S. Sanvito, Chem. Phys. **309**, 59 (2004).
[32] A. Filippetti, N. A. Spaldin, and S. Sanvito, J. Magn. Magn. Mater. **290-291**, 1391 (2005).

[33] T. C. Schulthess, W. M. Temmerman, Z. Szotek, W. H. Butler, and G. M. Stocks, Nat. Mater. **4**, 838 (2005).

[34] T. C. Schulthess, W. M. Temmerman, Z. Szotek, A. Svane, and L. Petit, J. Phys.: Condens. Matter **19**, 165207 (2007).

[35] J. Okabayashi, A. Kimura, T. Mizokawa, A. Fujimori, T. Hayashi, and M. Tanaka, Phys. Rev. B **59**, R2486 (1999).

[36] J. S. Blakemore, J. Appl. Phys. **44**, 3352 (1973).

[37] V. F. Masterov, S. B. Mikhrin, B. E. Samorukov, and K. F. Shtel'makh, Fiz. Tekh. Poluprovodn. **17**, 1259 (1983) [Sov. Phys. Semicond. **17**, 796 (1983)].

[38] T. Jungwirth, J. Sinova, A. H. MacDonald, B. L. Gallagher, V. Novák, K. W. Edmonds, A. W. Rushforth, R. P. Campion, C. T. Foxon, L. Eaves, E. Olejník, J. Mašek, S.-R. E. Yang, J. Wunderlich, C. Gould, L. W. Molenkamp, T. Dietl, and H. Ohno, Phys. Rev. B **76**, 125206 (2007).

[39] m is the 1×1 mass matrix describing the constrained motion of *all* nuclei.

[40] N. F. Mott and E. A. Davis, Philos. Mag. **17**, 1269 (1968).

[41] J. Zittartz, Phys. Rev. **164**, 575 (1967).

[42] T. Wojtowicz, T. Dietl, M. Sawicki, W. Plesiewicz, and J. Jaroszynski, Phys. Rev. Lett. **56**, 2419 (1986).